

Correlation Differences in Heartbeat Fluctuations During Rest and Exercise

Roman Karasik¹, Nir Sapir¹, Yosef Ashkenazy², Plamen Ch. Ivanov^{3,4},
Itzhak Dvir⁵, Peretz Lavie⁶, and Shlomo Havlin¹

¹ *Department of Physics and Gonda-Goldschmied-Center for Medical Diagnosis,
Bar-Ilan University, Ramat-Gan 52900, Israel*

² *Center for Global Change Science, Massachusetts Institute of Technology,
MIT Room 54-1726, Cambridge, MA 02139, USA*

³ *Center for Polymer Studies and Department of Physics, Boston University, Boston, MA 02215, USA*

⁴ *Harvard Medical School, Beth Israel Deaconess Medical Center, Boston, MA 02215, USA*

⁵ *Itamar Medical Ltd. Cesarea, Israel*

⁶ *Sleep Laboratory, Faculty of Medicine, Technion-Israel Institute of Technology, Haifa, Israel*
(November 6, 2018)

We study the heartbeat activity of healthy individuals at rest and during exercise. We focus on correlation properties of the intervals formed by successive peaks in the pulse wave and find significant scaling differences between rest and exercise. For exercise the interval series is anticorrelated at short time scales and correlated at intermediate time scales, while for rest we observe the opposite crossover pattern — from strong correlations in the short-time regime to weaker correlations at larger scales. We suggest a physiologically motivated stochastic scenario to explain the scaling differences between rest and exercise and the observed crossover patterns.

PACS numbers: 87.19.Hh, 05.45.Tp, 89.75.Da

One of the important questions in the analysis of complex physiological time series is how such series reflect the dynamical properties associated with the underlying control mechanism [1,2]. Recently, it was found, e.g., that the fluctuations of the heart interbeat intervals reveal long-range power-law correlations [3] and hidden scale-invariant structure [4] which may be useful for diagnosis and prognosis [5]. Here we study the correlation (scaling) properties of heartbeat dynamics as reflected by the pulse wave measured from the finger [6,7].

Previous studies of long interbeat interval series have focused primarily on 24h [8] and 6h [9] records, which include periods of rest as well as periods of a more intensive physical activity. However, heartbeat dynamics can change dramatically with physical activity. Thus important differences in cardiac regulation associated with rest and exercise may not be clearly seen when analyzing records which mix together rest and exercise regimes. Here we consider rest and exercise activities *separately*. We focus on the correlations in the interpulse interval (*IPI*) series derived from the pulse wave signal during rest and exercise (Fig. 1a). By studying the changes in the correlation properties we wish to achieve a better understanding of the physiological mechanism that regulates heartbeat dynamics at rest and during physical exercise.

We analyze 21 records from healthy subjects. Each record includes 4 different stages of physical activity denoted as *rest1*, *exercise1*, *rest2* and *exercise2* (Fig. 1b). At the first stage (*rest1*) we measure the *IPI* under normal rest conditions. At the next stage (*exercise1*) subjects are asked to run on a treadmill. After a short *recovery*, during which subjects sit down to recover their heart rate, a new rest-exercise episode (denoted as *rest2* and *exercise2*) is followed.

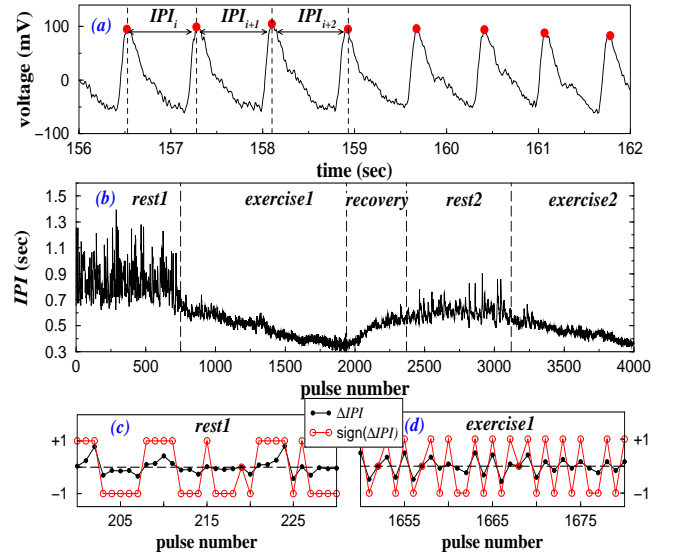


FIG. 1. (a) A typical example of a pulse wave measured as a function of time. As in the case of the electrocardiogram signal where interbeat interval fluctuations are studied (see, e.g., [8]), we analyze the interpulse intervals (*IPI*) between successive peaks in the pulse wave. (b) *IPI* series obtained from the pulse wave signal shown in (a). Each record includes two rest and two exercise stages. The duration of each stage varies from subject to subject and is between 6-10 minutes. (c) Sign series obtained from the increments ΔIPI in the interpulse intervals during rest and (d) during exercise. Note that the sign series of the exercise regime exhibits more frequent alternations (stronger anticorrelated behavior) compared to rest.

To study the correlation properties of the *IPI* series during rest and exercise stages we use the detrended fluctuation analysis (DFA) [10] which is a method developed

to avoid spurious detection of correlations that are artifacts of trends related to nonstationarity. The DFA procedure consists of the following steps. We first integrate the IPI series to construct the profile $Y(k) = \sum_{i=1}^k (IPI_i - \langle IPI \rangle)$ where $\langle IPI \rangle$ is the series average. Next, we divide the integrated signal, $Y(k)$, into equal windows of size n and find the local trend in each window by a least-squares polynomial fit. The order of the polynomial fit specifies the order of the DFA [11,12]. Then we calculate the average of the square distances around the local trend. This procedure is repeated to obtain the root mean square fluctuation function $F(n)$ for different window sizes n . A power-law relation between $F(n)$ and n , $F(n) \sim n^\alpha$, indicates the presence of scaling in the series. According to random walk theory, the scaling exponent α is related to the autocorrelation function exponent γ ($C(n) \sim n^{-\gamma}$ when $0 < \gamma < 1$) and to the power spectrum exponent β ($S(f) \sim 1/f^\beta$) by $\alpha = 1 - \gamma/2 = (\beta + 1)/2$ [13]. The value $\alpha = 0.5$ indicates that there are no (or finite-range) correlations in the data. When $\alpha < 0.5$ the signal is *anti-correlated*, meaning that large values are most probable to be followed by small values. The case of $\alpha > 0.5$ indicates the existence of persistent behavior in the time series, meaning that large values are most probable to be followed by large values. The higher α is, the stronger are the correlations in the signal.

We also study the correlation properties of the sign series $sign(\Delta IPI)$ [14], derived from the IPI increments $\Delta IPI_i = IPI_{i+1} - IPI_i$ [15]. Fig. 1c and Fig. 1d show representative examples of sign series obtained from rest and exercise stages respectively. For exercise, the signs of IPI increments tend to alternate rapidly, indicating a strong anticorrelated behavior. At rest stage, on the other hand, the signs alternate every several points, and thus this dynamics may be characterized by a more correlated behavior.

Due to the fact that during exercise the IPI series exhibits strong short-range anticorrelations, we first integrate the IPI series for all rest and exercise episodes (in addition to the integration built in the DFA method), to avoid inaccurate estimation of the scaling exponents for exercise segments. Because of the apparent linear decrease of the IPI during the exercise stage (Fig. 1b), the extra integration introduces a parabolic trend. To eliminate the effect of this parabolic trend in the exercise stage, we perform 3rd order DFA [16] on the *integrated* IPI series. The integration procedure is not necessary for evaluating α for the rest episodes, since they exhibit correlated behavior [17].

In Fig. 2a we present the fluctuation function, $F(n)$, of the integrated IPI series [18] for rest and exercise segments of a typical subject. For all 21 individuals we observe a characteristic crossover around $n \approx 20$ where there is a change in the correlation behavior between

short and intermediate scales regimes. We denote the scaling exponent of the short-range regime as α_1 (estimated for scales $8 \leq n \leq 14$) and the scaling exponent of the intermediate regime as α_2 (estimated for $30 \leq n \leq 300$). The type of crossover is different for rest and exercise: for the rest $\alpha_1 > \alpha_2$, while for the exercise $\alpha_1 < \alpha_2$. The fluctuation functions for rest and exercise stages construct a “fish”-like curve (Fig. 2).

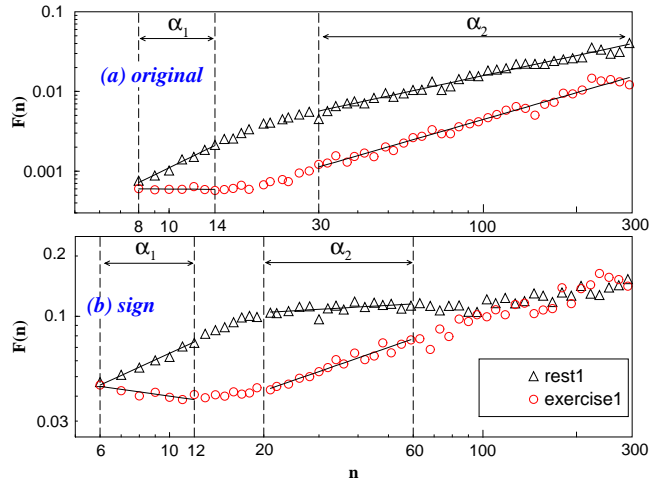


FIG. 2. Fluctuation function, $F(n)$, as a function of time scale n (in beat number) for rest (Δ) and exercise (\circ) stages of a typical healthy subject for (a) the original IPI series, and (b) the sign series $sign(\Delta IPI)$. For all records we observe a crossover between two different regimes of correlations. The dashed lines indicate the boundaries of these regimes in which short-range scaling exponents α_1 and intermediate exponents α_2 have been calculated. Note the different crossover patterns for rest ($\alpha_1 > \alpha_2$) and exercise ($\alpha_1 < \alpha_2$) stages.

We apply a similar scaling analysis to sign series derived from rest and exercise segments of the IPI signal (Fig. 2b). The sign series do not have any global trend, like the original IPI series have; thus, in this case it is enough to use 2nd order DFA. For sign series we calculate the short-range scaling exponent α_1 in the range $6 \leq n \leq 12$ and intermediate exponent α_2 in the range $20 \leq n \leq 60$ [20].

	original IPI series		$sign(\Delta IPI)$	
	α_1	α_2	α_1	α_2
<i>rest1</i>	1.42 ± 0.35	0.78 ± 0.16	0.47 ± 0.19	0.17 ± 0.11
<i>rest2</i>	1.43 ± 0.30	0.75 ± 0.17	0.38 ± 0.26	0.15 ± 0.12
<i>ex1</i>	-0.04 ± 0.26	1.07 ± 0.18	-0.17 ± 0.05	0.41 ± 0.09
<i>ex2</i>	-0.14 ± 0.17	1.11 ± 0.16	-0.21 ± 0.06	0.41 ± 0.1
<i>whole</i>	1.21 ± 0.25	0.91 ± 0.12	0.23 ± 0.15	0.22 ± 0.07

TABLE I. Comparison of scaling exponents α_1 and α_2 between rest stages, exercise stages and whole records that include rest and exercise episodes altogether. For each stage the average scaling exponent \pm standard deviation are shown.

We obtain a complete separation between rest and exercise for the original and sign series in the short range (Fig. 3) and an almost complete separation for the intermediate-range scaling exponents (Table I). The p -values for the original and sign series (obtained by the paired samples Student's t -test [19]) are less than 10^{-10} for the short-range regime and less than 10^{-4} for the intermediate regime. We find that our results are robust and do not change significantly with repetitive rest and exercise stages (Table I).

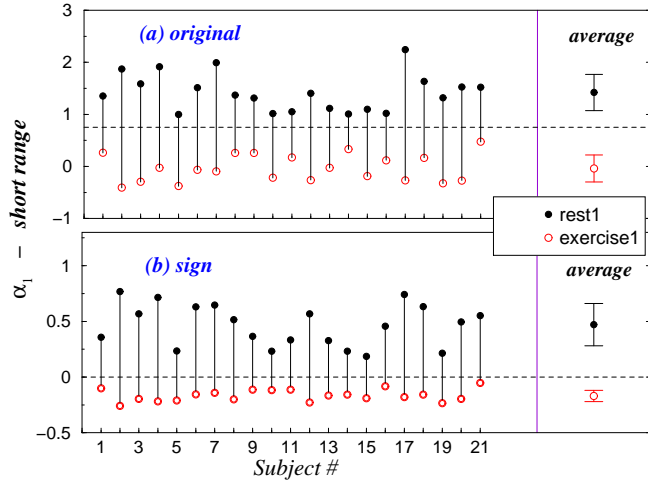


FIG. 3. Short-range scaling exponents α_1 from 21 healthy individuals (a) for the original IPI series and (b) for the sign series at rest (\bullet) and during exercise (\circ). At the right hand side we show the average $\alpha_1 \pm$ standard deviation. In accordance with Fig. 2, the short-range exponents during exercise are significantly smaller than during rest. Note the complete separation of the two stages, emphasized by the dashed lines.

To illustrate the importance of considering separately rest and exercise episodes, we perform our analysis also on the entire IPI records which include rest and exercise episodes altogether (Fig. 1b). We find indeed that the scaling of the whole record reflects neither the correlation properties of rest, nor of exercise (see Table I).

The significant differences between the values of α_1 (Fig. 3) and the different crossover patterns for rest and exercise stages (Fig. 2) may offer some insight on the underlying physiological mechanism controlling the heart-beat dynamics. The heart rhythm is regulated mainly by the parasympathetic (PS) and the sympathetic (SM) branches of the autonomic nervous systems [21]. PS impulses slow the heart rate while SM impulses accelerate it. The interaction between these two branches is reflected by the time organization of the IPI series (Fig. 1b).

The principle of homeostasis (dynamic equilibrium) asserts that physiological systems seek to maintain a constant output in spite of continuous perturbations [22]. However, healthy systems even at rest display highly irregular dynamics (see Fig. 1b) [1,2,25]. In a recent work Ivanov et al. [23] proposed a general approach based on

the concept of stochastic feedback to account for the complex fractal variability in biological rhythms. In this framework the time evolution of a physiologic system, e.g. the heartbeat dynamics, can be represented by a random walk biased toward some preferred “attracting” levels. Both the SM and PS systems controlling the heart rhythm generate attracting levels which bias the walker (modelling the interbeat interval series) in opposite directions leading to complex heart rate fluctuations. Although these attracting levels change in time, according to the response of the intrinsic physiological mechanism, they can vary in a limited range only, thus keeping the walker away from extreme values.

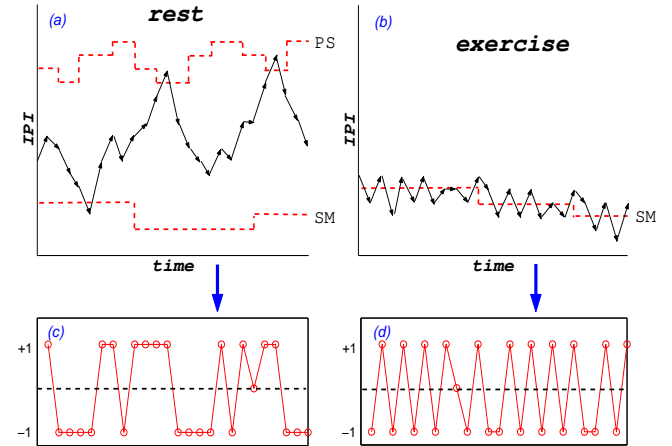


FIG. 4. Schematic illustration of a random walk with (a) two different levels of attraction and (b) a single attraction level, and their sign decomposition (c) and (d). (a) The combined effect of the upper level (representing the “preferred” level of parasympathetic (PS) system) and the lower level (sympathetic (SM) system) do not restrict the walker’s fluctuations for the short-time regime. But for the larger times the bounded walk results in a crossover to a less correlated behavior, similar to the crossover obtained for the rest stage (Fig. 2). (b) On the other hand, the walker attracted by a single SM level produces short-range anticorrelations with a crossover to a more correlated behavior in the intermediate regime due to the alterations of the SM level (mimicking exercise). The sign series for the two attractive levels presented in (c) is more likely to cluster than the series for a single level scenario presented in (d) (Compare with sign dynamics for rest and exercise shown in Fig. 1c and Fig. 1d).

Based on this general approach we suggest a schematic scenario that explains the different crossover patterns of the IPI fluctuations for rest and exercise (Fig. 2). At rest both the SM and PS systems are active, and each of them attracts the walker toward its own level (Fig. 4a). Since the response time of the PS system is shorter than that of the SM system [24,23], we assume that the preferred attracting level of the PS system alters more rapidly than the one related to the SM system. This scenario can account for the crossover observed for the rest stage

(Fig.2). When the walker is between the two attracting levels, each level imposes a bias in an opposite direction. Thus the walker is able to move in both directions until he crosses any of the two levels after which he is pulled back. This model scheme reproduces the crossover in the scaling behavior (Fig.2) from a larger value of the correlation exponent at short scales, where the fluctuations of the walker are not bounded, to a lower value of the exponent at large time scales, where the dynamics of the walker is bounded by the SM and PS attracting levels.

During exercise the SM system dominates [26] and the dynamics can be described effectively by a single attracting level (Fig.4b). In this case the walker fluctuates around this level producing an anticorrelated behavior at short time scales. However, since the attracting level changes with time and since the walker follows these changes, the fluctuations in the random walk increase at intermediate time scales, causing a crossover to a more correlated behaviour. This scheme accounts for the observed crossover pattern in the scaling of the IPI fluctuations from an anticorrelated behavior with small value of the correlation exponent at short time scales to a correlated behavior characterized by a larger value of the exponent at large time scales (Fig.2). Our scenario can also explain the remarkable difference in the amplitude of the fluctuations at rest and during exercise (see Fig.1b). When two attracting levels bias the walker (a situation in our scenario corresponding to rest) the fluctuations are larger compared to the exercise stage when there is a single dominant attracting level (Fig.4).

A “fish” structure similar to Fig. 2 (but with different scaling exponents) was observed when comparing healthy subjects with congestive heart failure patients [8]. These results support our scenario, since for heart failure patients there are evidences of SM dominance [27], resembling the state of the autonomic nervous system under physical exercise.

In summary, we study correlations in heartbeat fluctuations during rest and exercise. We show that the significant scaling differences and the different crossover patterns between rest and exercise (Fig. 2) can be explained based on the “attractive levels” scenario. We, therefore, conclude that the interaction between the competing branches of the autonomic nervous system underlies the correlation properties of heartbeat.

We wish to thank J.W. Kantelhardt and J.M. Hausdorff for helpful discussions. This work was supported by the Binational Israel-USA Science Foundation and the NIH/National Center for Research Resources (P41 RR13622).

- [1] J.B. Bassingthwaite, L.S. Liebovitch, B.J. West, *Fractal Physiology* (Oxford Univ. Press, Oxford, 1994).
- [2] M.F. Shlesinger and B.J. West, *Random Fluctuations and Pattern Growth: Experiments and Models* (Kluwer Academic Publishers, Boston, 1988);
- [3] C.-K. Peng *et al.*, Phys. Rev. Lett. **70**, 1343 (1993).
- [4] P.Ch. Ivanov *et al.*, Nature **383**, 323 (1996).
- [5] H.V. Huikuri *et al.*, Circulation **101**, 47 (2000); Y. Ashkenazy *et al.*, Europhys. Lett. **53**, 709 (2001).
- [6] Database provided by Itamar Medical Ltd (Cesarea, Israel) www.itamar-medical.com
- [7] R.P. Schnall *et al.*, Sleep **22**, 939 (1999).
- [8] C.-K. Peng *et al.*, Chaos **5**, 82 (1995).
- [9] P.Ch. Ivanov *et al.*, Europhys. Lett. **48**, 594 (1999).
- [10] C.-K. Peng *et al.*, Phys. Rev. E **49**, 1685 (1994).
- [11] 1st order DFA filters out constant trends in the time series, 2nd order DFA filters out linear trends etc.
- [12] A. Bunde *et al.*, Phys. Rev. Lett. **85**, 3736 (2000).
- [13] T. Vicsek, *Fractal Growth Phenomenon*, 2nd edn (World Scientific, Singapore, 1993).
- [14] Y. Ashkenazy *et al.*, Phys. Rev. Lett. **86**, 1900 (2001).
- [15] If, due to finite resolution, $\Delta IPI_i = 0$, we define $\text{sign}(\Delta IPI_i) = 0$.
- [16] We found that scaling exponents calculated using 4th order DFA are very close to the exponents obtained by 3rd order DFA. This indicates that we have reached the “real” scaling which is not an artifact of the global trend during exercise.
- [17] We applied DFA directly on non-integrated IPI series at rest and found that the results are very close to those obtained using the extra integration (see [18] for details).
- [18] We denote α as the scaling exponent for the original non-integrated signal. The integration of a signal increases the value of α by 1; e.g., a random walk ($\tilde{\alpha} = 1.5$) is the integration of a white noise ($\alpha = 0.5$). Thus, we divide the fluctuation function of the integrated IPI series $\tilde{F}(n)$ by the window size \tilde{n} , to restore the original α :

$$F(n) \equiv \tilde{F}(n)/n \sim n^{\tilde{\alpha}}/n \sim n^{\alpha+1}/n \sim n^{\alpha}$$
- [19] W.H. Press, S.A. Teukovsky, W.T. Vetterling, F.P. Flannery, *Numerical Recipes in C* 2nd ed. (Cambridge Univ. Press, 1996).
- [20] The differences in ranges of scaling exponents between original IPI series and $\text{sign}(\Delta IPI)$ are due to a shift in the crossover position, caused by applying higher order DFA. For large time scales sign series become uninformative indicating an uncorrelated behavior [14], forcing us to limit the upper boundary of the intermediate range to 60 beats.
- [21] R.M. Berne and M.N. Levy, *Cardiovascular Physiology*, 8th ed. (Mosby, St. Louis, 2000).
- [22] C. Bernard, *Les Phénomènes de la Vie* (Paris, 1878).
- [23] P.Ch. Ivanov *et al.*, Europhys. Lett. **43**, 363 (1998).
- [24] H.R. Warner and A. Cox, J. Appl. Physiol. **17a**, 349 (1962).
- [25] S. Akselrod *et al.*, Science **213**, 220 (1981).
- [26] B.F. Robinson *et al.*, Circ. Res. **19**, 400 (1966).
- [27] J.P. Saul *et al.*, Am. J. Cardiol. **61**, 1292 (1988).